Diffraction measurement and analysis of slanted holographic polymer dispersed liquid crystal

Xiao Hong Sun
Institute of Textiles and Clothing, The Hong Kong Polytechnic University, Hung Hom, Kowloon, Hong Kong and Department of Physics, University of Science and Technology of China, Hefei, Anhui 230026, China

Xiao Ming Tao,[a] Ting Jin Ye, Yau-Shan Szeto, and Xiao Yin Cheng
Institute of Textiles and Clothing, The Hong Kong Polytechnic University, Hung Hom, Kowloon, Hong Kong

(Received 21 February 2005; accepted 8 July 2005; published online 19 August 2005)

In this article, slanted holographic polymer dispersed liquid-crystal films are prepared by using a single-prism interferometer. Their diffraction characteristics are measured at various incident angles. Based on the coupled-wave theory of diffraction efficiency and incident angles, the grating period, film thickness, and slanted angle of the volume grating are derived. A good agreement is demonstrated between the experimental and theoretical results, and supported by scanning electron microscopy observation. The electrical switching behavior of the grating is also described. The diffraction efficiency changes from 65% to a stable value of 10% at an electric field of 33 V/μm. On the other hand, based on the theoretical prediction of diffraction efficiency, the optimum film thickness and Bragg grating period are determined, which sheds light on the implementation of our experiments. © *2005 American Institute of Physics*. [DOI: 10.1063/1.2010618]

I. INTRODUCTION

The development of holographic and diffractive optics technologies is of considerable interest for integrated optics, sensor systems, head-up displays, optical interconnects, optical data storage, and optical computers. In many applications it is desirable to have control over the diffraction efficiency of devices to obtain, for example, reprogrammable interconnects, angle multiplexers, electro-optically addressable volume data storage, fiber-optic switches, and dynamically variable focal length lenses. A promising approach is to employ holographic polymer dispersed liquid crystal (HPDLC) due to the large field-induced birefringence change in these materials. Switchable HPDLC are the subject of significant current interest.[1–7] HPDLC may have a horizontal multilayered structure and a perpendicular structure. In their study,[1,8] Sutherland *et al.* describe the permanent, but electrically switchable HPDLC gratings. The information storage characteristics of HPDLC with a perpendicular structure were investigated.[9,10] The HPDLC devices with a horizontal multilayered structure were studied.[4]

Recently many research groups are optimizing and evaluating new materials, exposure times, and preparation procedures[11–16] to achieve better reflection or diffraction efficiencies, lower switching voltages, and shorter response times.

In this article, slanted HPDLC gratings are fabricated with a different PDLC composite material. Their diffraction characteristics and electrical switching characteristics are investigated. Based on the coupled-wave theory, fitting of diffraction efficiency and incident angles, the grating period, film thickness, and slanted angle of the volume grating are derived. A good agreement is demonstrated between the experimental and theoretical results. On the other hand, the theoretical calculation of diffraction efficiency is also presented in terms of diffraction angles and film thickness. The optimum film thickness and Bragg grating period are identified.

II. EXPERIMENT

A. Materials and preparation of PDLC cells

Commercially available chemical reagents used are as follows: (1) liquid crystal (E7, Merck Inc), (2) divinyl ether of triethyleneglycol (RapiCure DVE-3 from International Speciality Products, 98%, Inc., USA) as a reaction diluent, and (3) a hydroxyphenyl ketone photoinitiator (Darocur 1173 from Ciba).

The synthesis of the allyl-ether-modified unsaturated polyesters (AUPEs) was conducted in our laboratory, shown in Fig. 1. For a typical reaction, 0.05 g of *p*-toluene sulfonic acid as a catalyst and 0.5 g of hydroquinone, used as an inhibitor, were put into a 250-mL three-necked flask with a mechanical stirrer, rectifying column, and purging system. The mixture was heated to 160 °C in an oil bath and refluxed for 3 h with the mechanical stirring (stirring speed was approximately 200 rpm). The temperature of the bath was

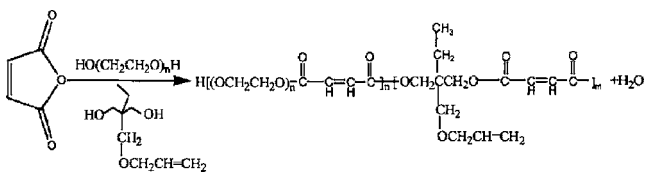

FIG. 1. Synthesis of AE-modified unsaturated polyester (UPE).

[a]Electronic mail: tctaoxm@polyu.edu.hk

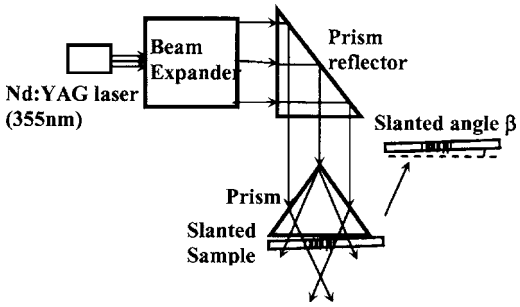

FIG. 2. Writing configuration of holographic gratings using the single-prism interferometer.

raised to 190 °C for 2 h. Then the reaction was performed in a vacuum of 40-mm Hg and at a temperature of 160 °C for 1 h to remove water in the system. The reaction was performed under N_2 atmosphere. The molecular weight of AUPE oligomer is 1674.

The emulsion was prepared by mixing the following components: 30% (by weight) nematic liquid-crystal mixture E7, 54% AUPE oligomer, 14% DVE-3 as a reactive diluent, and 2% Darocur 1173 as a photoinitiator. The components of the monomer mixtures and the LC were mixed homogeneously for 3 min in a glass vial at 60 °C. After mixing, the syrup was centrifuged for 1 min to remove dissolved gases. Indium-tin-oxide (ITO)-coated glass slides were cleaned with methanol prior to use. The 9-μm mylar spacers were utilized to ensure a uniform film thickness. After the PDLC film was holographically exposed, a continuous exposure under an ultraviolet lamp was applied for 5 min.

B. Grating writing by holographic exposure

In this study, strict darkroom conditions were used during the PDLC cell preparation. Holographic diffraction gratings were recorded by using a single-prism interfering system at a wavelength of 355 nm from a Nd: yttrium aluminum garnet (YAG) laser. The system configuration is shown in Fig. 2. By using a prism reflector, an expanded collimated laser beam was incident onto the apex of a prism with an angle of 90°, which acted as a beam splitter refracting the light on the both sides of the apex prism towards the cell. The cell was mounted under the hypotenuse of the prism. After taking an account for the optical losses, each beam had a power ranging from approximately 50 to 200 mW. The duration of exposure varied from 30 to 300 s. The typical exposure time was 90 s. After the holographic radiation, the photoinduced polymerization of the oligomers and phase separation led to the formation of a periodic structure, in which a polymer-rich and a liquid-crystal rich region alternatively distributed. A thin film is desirable because the voltage of electrical switching is approximately proportional to the film thickness. In order to reduce the switching voltage and to enhance the diffraction efficiency, the gratings were written at a slanted angle β.

The grating period of an unslanted grating[17] is

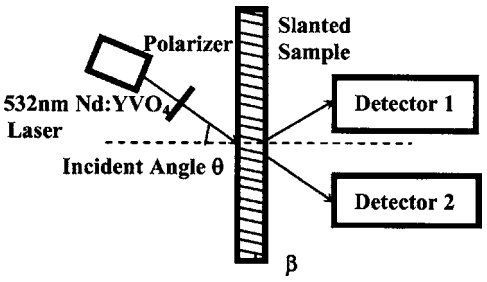

FIG. 3. The measurement system of peak diffraction efficiency at different angles.

$$\Lambda = \frac{\lambda_w}{2n_f n_a \sin[\alpha - \sin^{-1}(n_f^{-1} \sin \alpha)]}, \tag{1}$$

where λ_w(=355 nm) is the wavelength of the writing laser, $\alpha(=\pi/4)$ is the base angle, and n_f(=1.475 29) is the refractive index of the fused silica prism. n_a is the effective refractive index of the PDLC film calculated as $n_a = 30\% n_{\mathrm{LC}} + 70\% n_p = (30\%)\frac{1}{3}(2n_O + n_e) + 70\% n_p$. By substituting refractive indices of the liquid crystal $n_O = 1.5258$ and $n_e = 1.7366$ and that of the polymer $n_p = 1.485$ in the above mentioned equation, $n_a = 1.5183$ can be obtained. Hence $\Lambda = 281.5$ nm. Due to the slanted angle, the practical period on the film surface is $\Lambda' = \Lambda / \cos \beta$, where β is the slanted angle of the PDLC film.

C. Diffraction measurement

The measurement system of the peak diffraction efficiency is shown in Fig. 3. A 532-nm green Nd:YVO_4 laser was incident in the film at an angle θ to the film surface normal. The polarizer changed the *s*- and *p*-polarized directions of incident light. Detectors 1 and 2 were used to measure the Bragg diffraction and transmission intensity and obtain the diffraction efficiency. Assuming $\theta = 0$, the transmission intensity of *s*- and *p*-polarized light is $I_{s0} = 4.3$ mW and $I_{p0} = 1.8$ mW. The diffraction efficiency can be obtained by using I_{s0} or I_{p0} to divide the measured value of detector 1. The measured results of *s*- and *p*-polarized light are shown in small and large dots of Fig. 4, respectively. Because the gratings are slantedly written, when the light

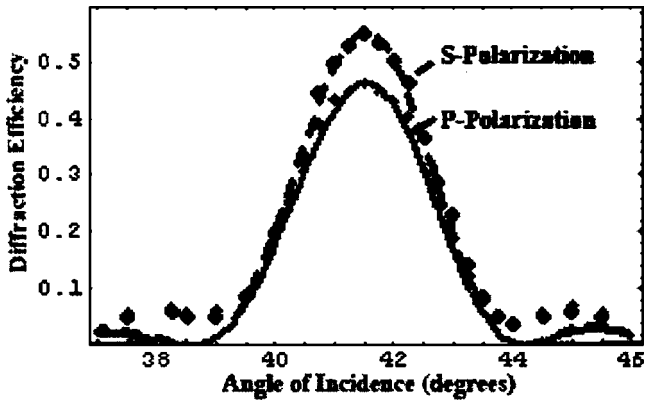

FIG. 4. Angular sensitivity plots for a PDLC-slanted grating written at 355 nm and read on the left side with 532 nm using *s*-polarization (large dots) and *p*-polarization (small dots) light. The solid and dashed curves are fits to the data using coupled-wave theory.

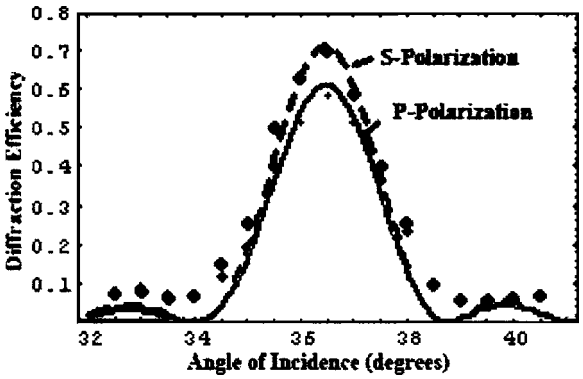

FIG. 5. Angular sensitivity plots for a PDLC-slanted grating read on the right side using *s*-polarization (large dots) and *p*-polarization (small dots). The solid and dashed curves are fits to the data using coupled-wave theory.

beam is incident on the right of the film (as shown in Fig. 3), the measured data are different from Fig. 4, shown in dots of Fig. 5.

D. SEM observation

Scanning electron microscopy (SEM) observations were carried out on a JEOL JSM-6335F field-emission SEM instrument. The films were prepared for SEM analysis first by peeling them from the glass substrate with a razor blade and removing the liquid crystal by immersing the free film in methanol for 12 h then drying at room conditions. The dried films were then mounted on metallic sample trays. A 205-nm-thick coating of gold was deposited on the surface of the specimen. Then the film was measured at a scanning voltage of 3 kV with different magnification amplitudes.

III. RESULTS AND DISCUSSION

A. Diffraction efficiency

From the coupled-wave theory,[18] the diffraction efficiency is given by

$$\eta = \frac{\sin^2(\nu^2 + \xi^2)^{1/2}}{\left(1 + \frac{\xi^2}{\nu^2}\right)}, \tag{2}$$

where $\nu = \pi n_1 L/\lambda \cos\theta$ for the *s*-polarized light and $\xi = \pi n L \Delta\theta \sin 2\theta/\lambda \cos\theta$. L is the physical thickness of the grating, n is the effective refractive index, n_1 is the amplitude of the index modulation (n_{1s} and n_{1p} for the *s*- and *p*-polarized light, respectively), λ is the reading wavelength, θ is the angle of incidence in the sample, and $\Delta\theta = \theta - \theta_B$ is the deviation from the Bragg angle θ_B.

The solid and dashed lines in Fig. 4 are fits of Eq. (2) to the measured diffraction efficiency and angle θ of *p*- and *s*-polarized light, assuming $n = 1.518$ and $\lambda = 532$ nm. The fitting results are $n_{1s} = 0.0204$, $n_{1p} = 0.0182$, $L = 5.2\ \mu$m, and $\theta_{B1} = 41.5°$. When the light beam is incident on the right of the film (as shown in Fig. 3), the measured data of the *s*- and *p*-polarized light are shown in Fig. 5 with large and small dots, and the fitting results are in line of Fig. 5. The *s*- and *p*-fitting lines are dashed and solid, respectively. The fitting results are $n_{1s} = 0.0204$, $n_{1p} = 0.0182$, $L = 6.7\ \mu$m, and $\theta_{B2} = 36.5°$. So the Bragg angle of the gratings should be $\theta_B = (\theta_{B1} + \theta_{B2})/2 = 39°$, and the slanted angle of gratings is $\beta = 2.5°$. Based on the Bragg diffraction equation $2n\Lambda \sin\theta_B = \lambda$, assuming $n = 1.518$ and $\lambda = 532$ nm, this gives a grating spacing of 281 nm. The ratio of the coupling coefficient of *p*-polarized and *s*-polarized light is $\nu_p/\nu_s = n_{1p}/n_{1s} = 0.89$. The value is larger than that of unslanted gratings. On the other hand, because the amplitude of the index modulation n_1 is large, the half-width angle of angular selectivity is also very large. The fitting results also tell us that we can increase the diffraction efficiency by decreasing the index modulation n_1 or increasing the refractive index of the polymer in PDLC.

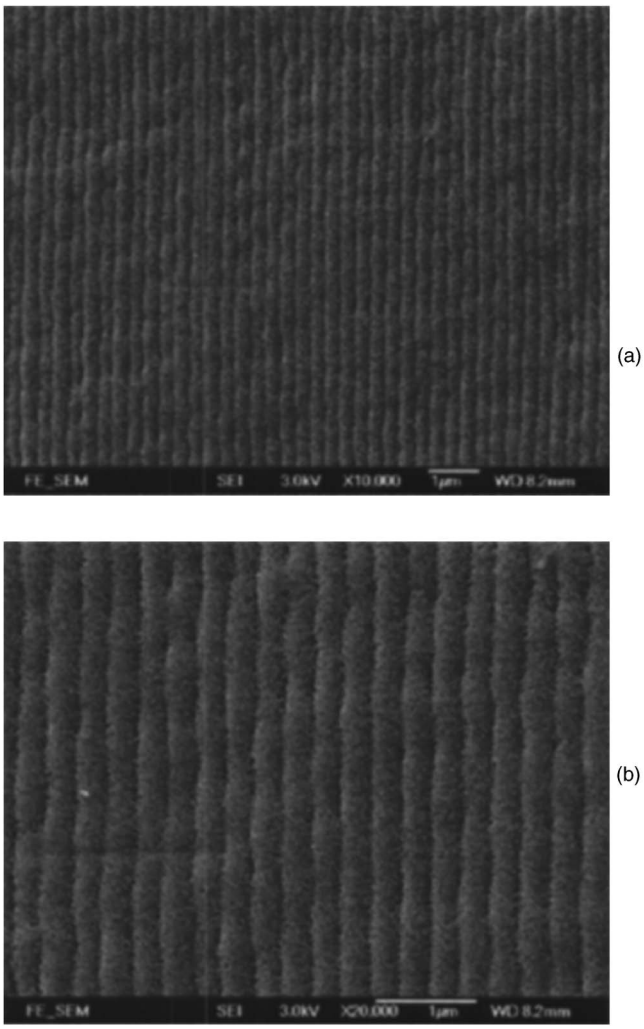

FIG. 6. SEM photographs of an in-plane view of a PDLC grating at a scanning voltage and magnification (a) at 3 kV and 10 000× and (b) at 3 kV and 20 000×.

B. SEM topography

Micrographs of SEM are shown in Figs. 6(a) and 6(b). The grating spacing is 285.7 nm and the average size of LC is 10 nm. Considering the slanted angle of 2.5°, the grating period is given as

$$\Lambda = 285.7 \cos 2.5^{\circ} = 285 \text{ nm}.$$

There is an excellent agreement between the SEM measured value, the diffraction measurement result (281 nm), and the

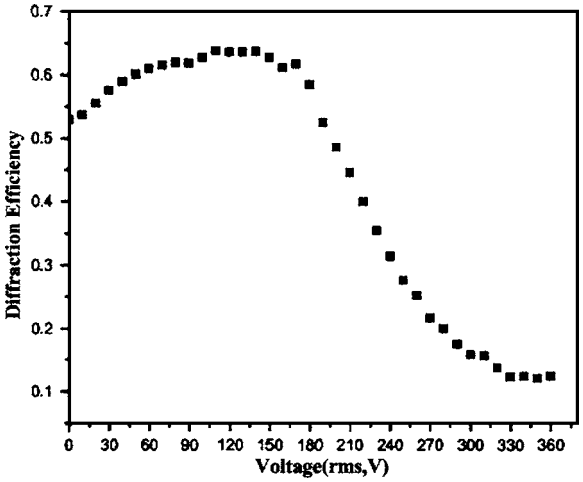

FIG. 7. *s*-polarized diffraction efficiency as a function of root-mean-square (rms) applied voltage

theoretical calculation from the geometry of our recording setup (281.5 nm).

C. Electrical switching

Electric-field control of the diffraction efficiency was measured as illustrated in Fig. 7. The grating was read with a *p*-polarized $Nd:YVO_4$ laser. The diffraction efficiency reaches an actual minimum (10%) at ~300 V (root-mean-square) or 33 V/μm (the sample thickness is 9 μm). This value of switch voltage is high. This is perhaps because the size of the LC is very small (~10 nm).

D. Optimum of film thickness and grating period

To obtain the highest diffraction efficiency, film thickness and Bragg grating period should be chosen appropriately. According to Eq. (2), the diffraction efficiency (h) is calculated as a function of film effective thickness (L) and Bragg angle (qB). Figure 8(a) shows the calculated result at 455-nm wavelength, which has a fluctuation and pseudoperiodic change at lower Bragg angles. To view the variation more clearly, a contour plot of the function is shown in Fig. 8(b). The lighter the color shade is, the larger the diffraction efficiency is. At point A where the largest diffraction efficiency occurs, the Bragg angle and film thickness are 20° and 10 μm, respectively. That is to say, a film sample, made

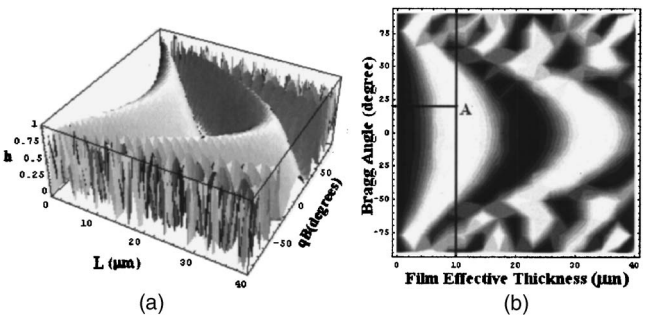

FIG. 8. (a) Diffraction efficiency (h) of λ=455-nm blue light changing with film effective thickness (L) and Bragg angle (qB). (b) The contour plot of (a): the more shallow the color is, the larger the diffraction efficiency is.

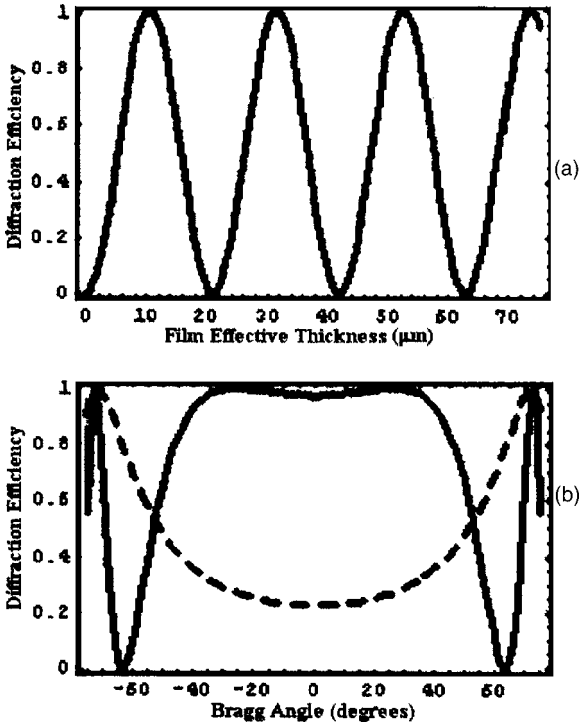

FIG. 9. (a) When Bragg angle is at 20°, the diffraction efficiency changes with film effective thickness periodically. (b) When the film thickness is equal to 10 μm (solid line) and 3.5 μm (dashed line), the diffraction efficiency changes with the Bragg angle.

of the current material system, with a grating period of 437.6 nm and thickness of 10 μm, has the largest diffraction efficiency when a blue light of 455 nm is incident at a Bragg angle of 20° ($2n\Lambda \sin \theta_B = \lambda$, $n=1.518$, and $\lambda=455$ nm).

Figure 9(a) shows the periodical change of diffraction efficiency with the film thickness at a Bragg angle of 20°. The period is 21 μm. Because of the near-periodical change of diffraction efficiency, another film sample with a thickness of 31 μm has the largest diffraction efficiency under the same incident conditions. The solid line at Fig. 9(b) indicates that when the film thickness is 10 μm, the Bragg diffraction

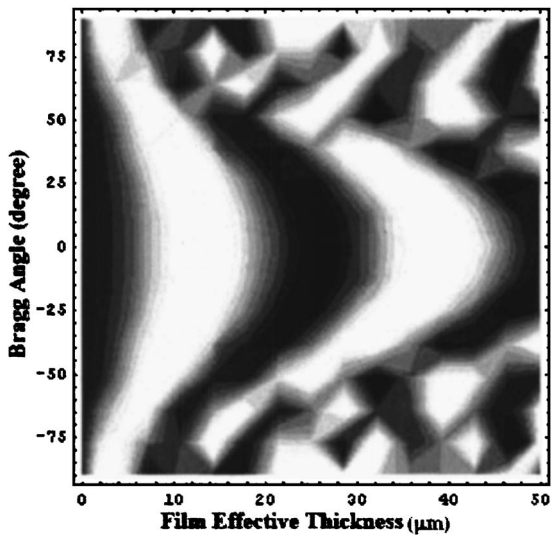

FIG. 10. Contour plot of the diffraction efficiency of λ=532-nm green light vs film thickness and Bragg angle.

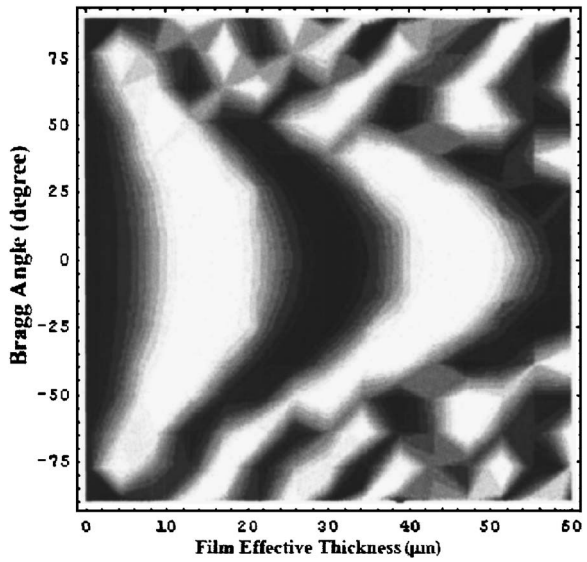

FIG. 11. Contour plot of the diffraction efficiency of $\lambda = 632$-nm red light vs film thickness and Bragg angle.

angle (grating period) influences the diffraction efficiency. In a wide range of Bragg angles (from $-40°$ to $40°$), the diffraction efficiency is almost 1. This can decrease the limitation to the grating period and easily realize large diffraction efficiency. Furthermore, Fig. 8 shows that if the sample thickness is less than 4 μm, it is difficult for the 455-nm blue light to obtain the full diffraction efficiency. The dashed line at Fig. 9(b) shows the change of diffraction efficiency at a film thickness of 3.5 μm. In a wide range of angles, the diffraction efficiency is below 30%.

In a similar manner, the diffraction efficiency of the 532-nm green light and the 632-nm red light are calculated and their contour plots are shown in Figs. 10 and 11, respectively. As the wavelength of the incident light increases, with an identical Bragg angle, say $20°$, the optimum thickness increases as the highest diffraction peak moves towards the right side. Comparing 10 μm with the incident light of 455 nm, the optimum thickness with a Bragg angle of $20°$ is approximately 14 and 16 μm at 532 and 632 nm, respectively.

Hence, on one hand, based on the sample thickness and grating period, the diffraction efficiency of different wavelengths can be obtained from Figs. 8(b), 10, and 11. On the other hand, given the diffraction efficiency and Bragg angle, the film thickness and grating period can be determined.

IV. CONCLUSIONS

In this article, slanted holographic polymer dispersed liquid-crystal films have been prepared by using the single-prism interferometer. Diffraction characteristics at different incident angles have been measured. Based on the coupled-wave theory of diffraction efficiency and incident angles, the grating period, film thickness, and slanted angle of volume grating are obtained. A good agreement is acquired between the SEM measurement (285 nm), the diffraction measurement result (281 nm), and the theoretical calculation from the geometry of our recording setup (281.5 nm). The diffraction efficiency of Electrical switching of is also determined. The diffraction efficiency can be switched from a value of 65% to a stable value at fields ~ 33 V/μm. Based upon the calculation of diffraction efficiency with diffraction angles and film thickness, the optimum film thickness and Bragg grating period are identified. This will provide an important guide for experimental investigation.

ACKNOWLEDGMENTS

The authors wish to acknowledge the funding support from the Research Grants Council (PolyU5152/01E) and Innovation and Technology Commission (ITS/071/02), the Hong Kong SAR Government.

[1] R. L. Sutherland, L. V. Nataranjan, V. P. Tondiglia, and T. J. Bunning, Chem. Mater. **5**, 1533 (1993).
[2] T. J. Bunning, L. V. Nataranjan, V. P. Tondiglia, and R. L. Sutherland, Annu. Rev. Mater. Sci. **30**, 83 (2000).
[3] T. J. Bunning, L. V. Nataranjan, V. P. Tondiglia, R. L. Sutherland, and W. W. Adams, Polymer **36**, 2699 (1995).
[4] A. Y.-G. Fuh, T.-C. Ko, M.-S. Tsai, C.-Y. Huang, and L.-C. Chien, J. Appl. Phys. **83**, 679 (1998).
[5] C. C. Bowley, P. A. Kossyrev, G. P. Crawford, and S. Faris, Appl. Phys. Lett. **79**, 9 (2001).
[6] M. Jazbinsek, I. D. Olenik, M. Zgonik, A. K. Fontecchio, and G. P. Crawford, J. Appl. Phys. **90**, 3831 (2001).
[7] C. C. Bowley and G. P. Crawford, Appl. Phys. Lett. **76**, 2235 (2000).
[8] R. L. Sutherland, V. P. Tondiglia, and L. V. Natarajan, Appl. Phys. Lett. **64**, 1074 (1994).
[9] A. Y.-G. Fuh, C.-Y. Huang, M.-S. Tsai, J.-H. Chen, and L.-C. Chien, Jpn. J. Appl. Phys., Part 1 **35**, 630 (1996).
[10] K. Tanaka, K. Kato, S. Tsuru, and S. Sakai, SID Int. Symp. Digest Tech. Papers **25**, 37 (1994).
[11] K. Kato, T. Hisaki, and M. Date, Jpn. J. Appl. Phys., Part 1 **38**, 1466 (1999).
[12] L. V. Natarajan, R. L. Sutherland, V. P. Tondiglia, T. J. Bunning, and R. M. Neal, Proc. SPIE **3143**, 182 (1997).
[13] L. H. Domash *et al.*, Proc. SPIE **2689**, 188 (1996).
[14] F. Simoni, G. Cipparrone, A. Mazzulla, and P. Pagliusi, Chem. Phys. **245**, 429 (1999).
[15] Y. J. Liu, B. Zhang, Y. Jia, and K. S. Xu, Opt. Commun. **218**, 27 (2003).
[16] B. Zhang, Y. J. Liu, and Y. Jia, Acta Phys. Sin. **52**, 91 (2003).
[17] Q. Zhang, D. A. Brown, L. Reinhart, and T. F. Morse, Opt. Lett. **19**, 2030 (1994).
[18] H. Kogelnik, Bell Syst. Tech. J. **48**, 2909 (1969).